Journal of Superconductivity: Incorporating Novel Magnetism, Vol. 15, No. 5, October 2002 (© 2002)

Phonon Dispersion Measurements of $YBa_2Cu_3O_{6.15}$ and $YBa_2Cu_3O_{6.95}$ by Time-of-Flight Neutron Spectroscopy

J.-H. Chung,[1] T. Egami,[1] R. J. McQueeney,[2] M. Yethiraj,[3] M. Arai,[4] T. Yokoo,[4] H. A. Mook,[3] Y. Endoh,[5] S. Tajima,[6] C. Frost,[7] and F. Dogan[8]

We measured the phonon dispersions of $YBa_2Cu_3O_{6.15}$ and $YBa_2Cu_3O_{6.95}$ by time-of-flight inelastic neutron scattering. The in-plane bond-stretching modes in the metallic phase showed a distinct *a*-*b* plane anisotropy beyond what is expected for structural origin. Such anisotropy in the longitudinal optical modes, which is absent in the TO, suggests strong in-plane anisotropy in the underlying electronic structure. Apical oxygen bond-stretching modes showed a large frequency change between the insulating and the metallic phases. This large softening also is beyond structural origin, and suggests the effect of local electronic environment.

KEY WORDS: phonon dispersion; MAPS; Y-based cuprates; in-plane anisotropy.

1. INTRODUCTION

Interest in the phonons in high-T_C superconductors is on the rise because of recent discoveries of lattice anomalies in cuprates and related compounds [1–5]. One of the most conspicuous phonon anomalies is the zone-boundary softening of the in-plane oxygen bond-stretching longitudinal optical (LO) modes with doping [2–4]. Apical oxygen bond-stretching modes are also known for anomalies observed with optical spectroscopy [6–8]. Raman and IR spectroscopies suggested their zone-center phonon modification is more than of a simple structural or ionic origin. In this study, we used the chopper spectroscopy of pulsed neutrons for the measurement of phonon dispersions in $YBa_2Cu_3O_{7-\delta}$ (YBCO). By this method it was possible to take a "snapshot" of the whole dispersion with a fairly good resolution.

2. EXPERIMENT

The measurement was performed using the MAPS spectrometer at the ISIS facility of Rutherford Appleton Laboratory. The MAPS is a time-of-flight neutron chopper spectrometer with position sensitive detector (PSD) arrays, which provides a simultaneous access to a wide range of three-dimensional ω-$\boldsymbol{Q}$ space ($\boldsymbol{Q}$ in two-dimensions). Figure 1 schematically describes the geometry of the sample alignment with respect to the incoming neutron beam and the PSD panels. The *c*-axis of the tetragonal/orthorhombic sample was placed in the horizontal plane that includes the incoming neutron beam, k_i. The *c*-axis was then rotated by angle φ in order to optimize the *l*-index in the region of interest in energy transfer. We used two different alignments with $\varphi = 49^\circ$ and $\varphi = 90^\circ$, focusing on in-plane and out-of-plane displacements, respectively. With $\varphi = 49^\circ$, *l* index is ~0 at ($h = 3, k = 0$) and 50 meV, and ~2.0 at (3, 0) and

[1]Department of Materials Science and Engineering, University of Pennsylvania, Philadelphia, Pennsylvania 19104.
[2]Los Alamos National Laboratory, Los Alamos, New Mexico 87545.
[3]Oak Ridge National Laboratory, Oak Ridge, Tennessee 37831.
[4]Institute of Materials Structure Science, KEK, Tsukuba 305-0801, Japan.
[5]Institute for Materials Research, Tohoku University, Sendai 980, Japan.
[6]Superconductivity Research Laboratory, International Superconductivity Technology Center, Tokyo 135-0062, Japan.
[7]Rutherford Appleton Laboratory, Didcot, Oxon OX11 0QX, UK.
[8]Department of Materials Science, University of Washington, Seattle, Washington 98195.

0896-1107/02/1000-0327/0 © 2002 Plenum Publishing Corporation

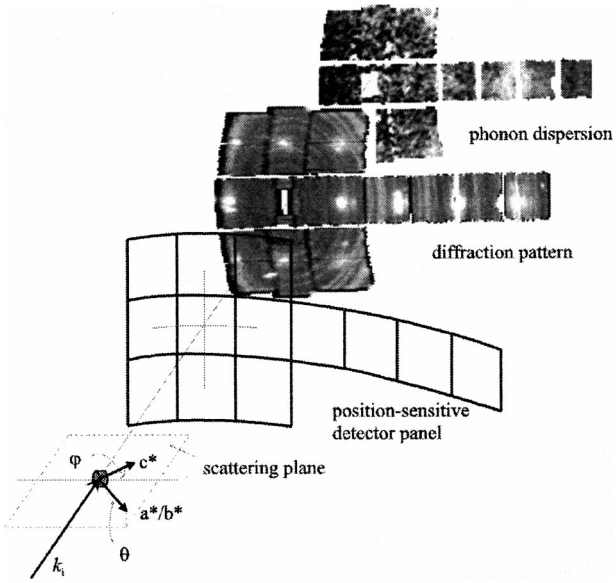

Fig. 1. The geometry of sample orientation with respect to the position sensitive detectors.

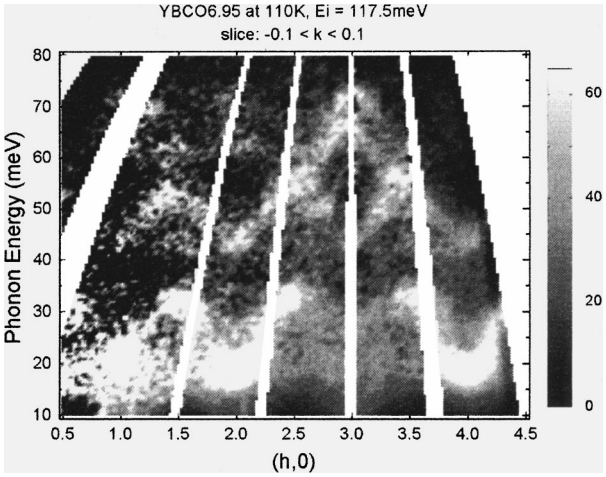

Fig. 2. S($\boldsymbol{Q}$, ω) measured from $YBa_2Cu_3O_{6.95}$ at $\varphi = 49^\circ$. In this cut, the observed intensity is mostly from in-plane longitudinal components.

70 meV.[9] Under this setting we measure mostly in-plane displacements, since the neutron scattering intensity is proportional to $(\boldsymbol{Q} \cdot \varepsilon)^2$, where ε is the phonon polarization [9]. With $\varphi = 90^\circ$, l index is ~2.0 at (1, 0) and 50 meV, and ~4.0 at (1, 0) and 70 meV, measuring mostly out-of-plane displacements. Either a- or b-axis was placed within the horizontal plane in order to project one of crystallographic principal axes along the extended wing of the PSD panel. For the maximum availability of in-plane transverse modes, the sample was rotated by a small amount around the c-axis.

Flux-grown single crystals were used for the measurement, which have been well characterized and used for numerous previous reports [10]. For the optimally doped sample ($YBa_2Cu_3O_{6.95}$), which contained twins of equal proportion, data were taken with two different sample orientations, $\varphi = 49^\circ$ and $\varphi = 90^\circ$. For the insulating sample ($YBa_2Cu_3O_{6.15}$), so far the data were taken only with $\varphi = 49^\circ$. The sample temperature was 7 K and 110 K. The raw intensity data in the (ω, h, k, l) coordinate system were corrected for the energy-dependent background, which consists mostly of the multiphonon intensity, and were multiplied by $\omega/\boldsymbol{Q}^2$ and the Debye–Waller factor to extract the one-phonon scattering factor, or the dynamic structure factor S($\boldsymbol{Q}$, ω). The dynamic structure factor extracted in such a way was then integrated along the l-direction, and plotted on the two-dimensional plane of frequency versus h/k for visualization. Figure 2 shows S($\boldsymbol{Q}$, ω) obtained from the optimally doped sample at $\varphi = 49^\circ$ in the longitudinal configuration. The experimental phonon dispersions were extracted by harmonic model fits to constant-$\boldsymbol{Q}$ cuts. The instrumental energy resolution was about 4 meV at 40 meV energy transfer, and 3 meV at 80 meV. During the peak-fitting procedure slightly wider resolutions (~30%) were assumed to maintain the consistency between different $\boldsymbol{Q}$-cuts and to avoid the error due to statistical noise or spurious intensities. No additional sample broadening was considered at this stage.

[9] As we neglect the l-dependence of spectrum, (h, k) notation without l is used throughout the report.

3. RESULTS AND DISCUSSIONS

3.1. In-Plane Oxygen Modes in the Optimally Doped Sample

Although the sample was twinned, the orthorhombic splitting at the zone center allowed us to identify the in-plane anisotropy. We find that the higher mode at 72 meV is polarized along the a-direction and the lower mode at 66 meV along the b-direction. The frequency and the split agree very well with the result from Raman spectroscopy [11]. The dispersions and assignments for high-energy modes

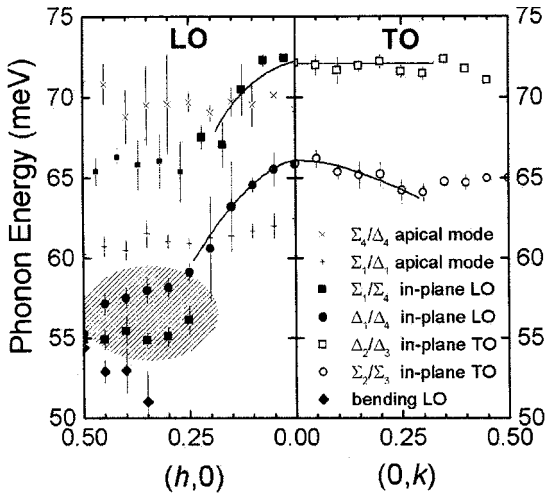

Fig. 3. Experimental dispersion curves from $YBa_2Cu_3O_{6.95}$ at 110 K. There is no apparent change of dispersion at 7 K. The shaded area indicates the modes resolved assuming resolution better than reality. Small markers indicate relatively weak intensity peaks. The solid lines are guide to the eye.

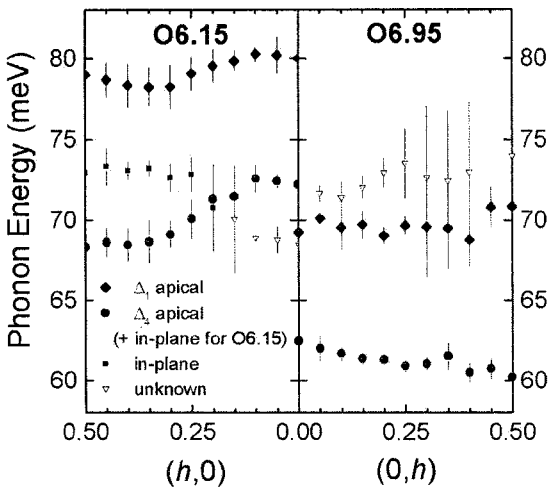

Fig. 4. Experimental dispersion curves for modes with large apical components.

are shown in Fig. 3. The dispersion and intensity of the two in-plane modes showed very different behaviors beyond $q \sim (0.25, 0)$. Most importantly, the intensity of the $\Sigma\,(= a)$ LO branch rapidly decreased beyond $(0.25, 0)$, while the $\Delta\,(= b)$ LO branch mixed with an intense flat mode around 55 meV near the zone boundary, which we identified as the second Σ LO branch. Such split dispersion has been observed for $La_{1.85}Sr_{0.15}CuO_4$ [4], and suggested for $YBa_2Cu_3O_{7-\delta}$ [5] as well. The presence of split dispersion only for the Σ mode as observed in this study is consistent with the stripe picture of modulated periodicity along the a-direction [5]. The detailed account of the anisotropy is discussed in a separate publication [10].

3.2. Apical Oxygen Modes

The dispersions and assignments of apical oxygen modes for the insulating and the optimally doped samples are shown in Fig. 4. As we have only one data set for the insulating phase, its assignment is not conclusive. The zone center frequencies agreed very well with optical spectroscopy [7,8]. The most noticeable difference between the two samples was the overall softening, as large as 10 meV for both modes, which is even larger than the calculation with isotropic screening [12]. Thus, it is likely that the oversoftening of these modes is beyond normal structural and ionic effects. The anomaly of the apical oxygen vibrations near the insulator/metal boundary is demonstrated by the Raman and IR results that these modes form double peaks in the intermediate doping range without continuous softening [7,8]. Therefore, it is very likely that the apical oxygen vibration is predominantly determined by the local electronic environment.

3.3. Temperature Dependence

The dispersions of the bond-stretching phonon branches appeared to show no clearly identifiable temperature dependence. But the scattering intensity was found to show substantial changes beyond what is expected for thermal excitation. For the in-plane modes, a detailed account is given in another publication [10]. The apical oxygen modes also showed their own share of temperature dependence. The analysis of the intensity of the apical mode of Δ_1 symmetry suggested that the eigenvector becomes more planar at low temperature. This temperature dependence is consistent with the change of interaction strength within and perpendicular to the plane. If that is the case, it may be explainable with the stripe picture where the ordering of charges can induce changes in interaction strength as well as bond distance.

ACKNOWLEDGMENTS

This work was supported by the National Science Foundation through DMR01-02565.

REFERENCES

1. T. Egami and S. J. L. Billinge, in *Physical Properties of High Temperature Superconductors V*, D. Ginsberg, ed. (Singapore, World Scientific, 1996) p. 265.
2. L. Pintschovius, N. Pyka, W. Reichardt, A. Yu. Rumiantsev, N. L. Mitrofanov, A. S. Ivanov, G. Collin, and P. Bourges, *Physica C* (*Amsterdam*) **185–189,** 156 (1991).
3. R. J. McQueeney, Y. Petrov, T. Egami, M. Yethiraj, G. Shirane, and Y. Endoh, *Phys. Rev. Lett*. **82,** 628 (1999).
4. Y. Petrov, T. Egami, R. J. McQueeney, M. Yethiraj, H. A. Mook, and F. Dogan, *Preprint* cond-mat/0003414 (2000).
5. H. A. Mook *et al.*, *Nature* (*London*) **404,** 729 (2000).
6. J. Schützmann, S. Tajima, S. Miyamoto, Y. Sato, and R. Hauff, *Phys. Rev. B* **52,** 13665 (1995).
7. R. M. Macfarlane, H. J. Rosen, E. M. Engler, R. D. Jacowitz, and V. Y. Lee, *Phys. Rev. B* **38,** 284 (1988).
8. G. Burns, F. H. Dacol, C. Field, and F. Holtzberg, *Physica C* **181** 37 (1991).
9. S. W. Lovesey, *Theory of Neutron Scattering from Condensed Matter, Vol. 1* (Clarendon Press, Oxford, 1984).
10. J.-H. Chung, T. Egami, R. J. McQueeney, M. Yethiraj, M. Arai, T. Yokoo, Y. Petrov, H. A. Mook, Y. Endoh, S. Tajima, C. Frost, and F. Dogan (manuscript submitted for publication).
11. K. F. McCarty, J. Z. Liu, R. N. Shelton, and H. B. Radousky, *Phys. Rev. B* **41,** 8792 (1990).
12. S. L. Chaplot, W. Reichardt, L. Pintschovius, and N. Pyka, *Phys. Rev. B* **52,** 7230 (1995).